Proceedings of the 28th IEEE
EMBS Annual International Conference
New York City, USA, Aug 30-Sept 3, 2006

Fundus Foveal Localization Based on Vessel Model

Opas Chutatape, *Senior Member, IEEE*

Abstract— **The problem of automatically locating the fovea, a spot located in the center of the macula and responsible for sharp central vision, on the retinal surface image is considered. The uniqueness of the strategy presented here is the relatively small amount of computational expense of a quick and robust method conducive to real-time applications. The algorithm first identifies the main blood vessels using the modified active shape model (ASM) and then expeditiously attempts to fit the parabolic shape to the overall result to locate the fovea. A reliable tracking strategy is also proposed here to estimate the required vertex when the prior information of the optic disk is not available. When a patient's retinal vessel data have been modeled *a priori* and used as template, the technique brought up here should find its advantage in real-time image-guided applications like a computer-assisted photocoagulation treatment.**

Index term: retinal image, ASM, foveal localization, vessel tracking

I. Introduction

Many research results on the analysis of color fundus image have been reported as reviewed in [1]. Some of the work tried to extract the anatomical structures such as optic disk, fovea and blood vessels. Others attempted to detect lesions including cotton-wool spot, exudates and hemorrhages to help the diagnosis. While most of the effort is put on improving the detection algorithm, one thing less mentioned is the distribution of the lesions. In fact the locations of lesions are as important as their size and number to ophthalmologists [2]. Therefore not only the detection but also the means to describe the spatial locations of the objects and the spatial relationship between them need to be investigated.

This paper describes how the location of the macula and fovea can be identified based mainly on the structure of blood vessels and with little information on the optic disk. A polar fundus coordinate system can be set up once the fovea location is identified. A descriptive method for the contents of fundus image can then be provided to facilitate the database establishment and the information transmission of fundus images. It could be equally important for further development in the computer-assisted photocoagulation treatment where the macula area must be carefully identified and treated. A concise description of this approach is given in the following sections.

Manuscript received April 4, 2006.
The author is with the Department of Electrical and Computer Engineering, College of Engineering, Rangsit University, Patumtani 12000, Thailand; e-mail: opas@rangsit.rsu.ac.th

II. Extracting the Main Structure of Blood Vessels

In a fundus image, the central retinal artery and vein normally appear close to each other at the nasal side of the center of optic disk. The vessels divide into a large superior and inferior branch and later into temporal and nasal branches to supply the fundus. The course is slightly sinuous and proceeds into many smaller branches. Three strategies have been employed to detect blood vessels: window-based, tracking-based and neural network. The window-based strategy [3] [4] includes two categories of edge detection methods: enhancement/ thresholding or edge fitting. In the category of enhancement/thresholding, the edges in the gray image are enhanced by neighborhood operators and later a threshold is selected to segment the blood vessels [3]. The edge fitting methods take into account special properties of blood vessels and use the rotated matched filters to detect piecewise linear segments of blood vessels [4][15]. One of the special properties of the blood vessels considered is that the two edges of a vessel always run parallel to each other, which is referred to as 'anti-parallels'. It is difficult for the window-based strategy to detect small vessels without fragmentation results when the contrast between vessels and the retinal background is low. Another strategy is vessel tracking [6] [7] [8] [9]. The strategy works by first locating an initial point and then exploiting local image properties to trace the vessels. The starting points can either be at the optic disk or at the subsequently detected branching points. The strategy can provide a meaningful description of the vessel network, but the drawback is its proclivity for termination at the branching points.

Neural Network was employed to classify the objects in the fundus image [10] [11]. The back propagation neural network was trained to classify the small sub-images as retinal background, vessels, exudates, or hemorrhages in [11]. The whole square was classified as blood vessel, which was a rough detection of blood vessels. Each pixel was classified as vessel or non-vessel according to the first principal component of the color components and the edge strength in its sub-images in [10]. The method did not consider the images with lesions where hemorrhages are similar to blood vessels.

1-4244-0033-3/06/$20.00 ©2006 IEEE.

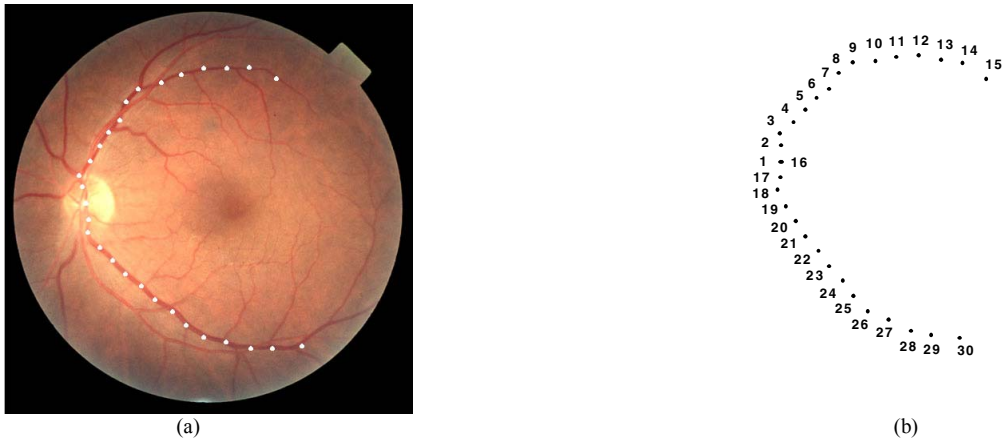

(a) (b)

Figure 1: Landmark points of blood vessels on one of the training images

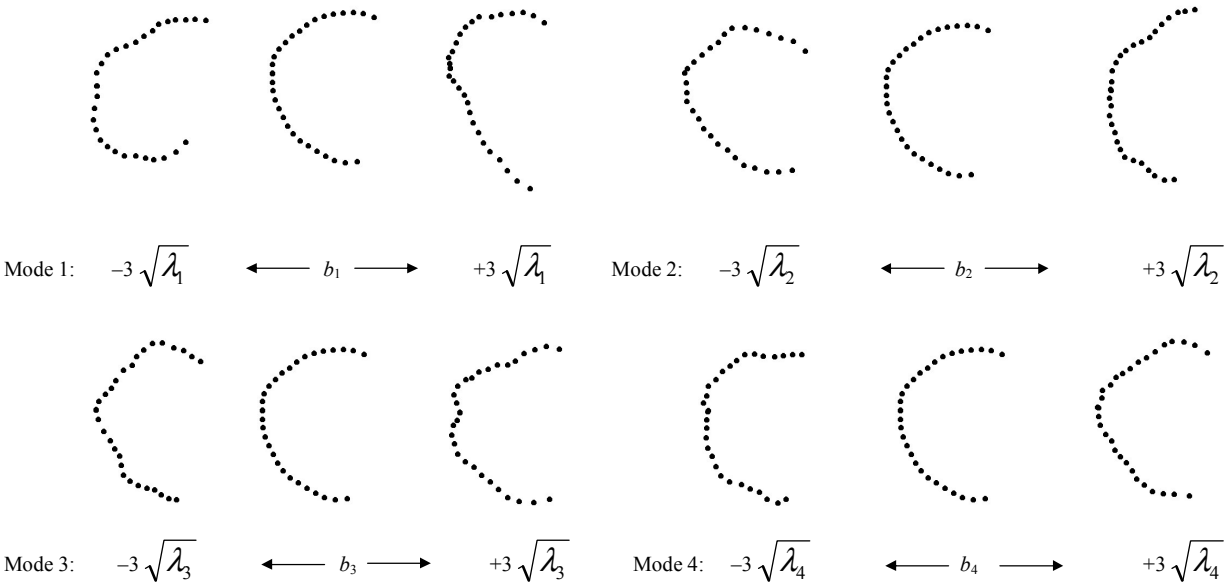

Figure 2: The first four modes of variation from –3 to +3 standard deviation in the model of blood vessels

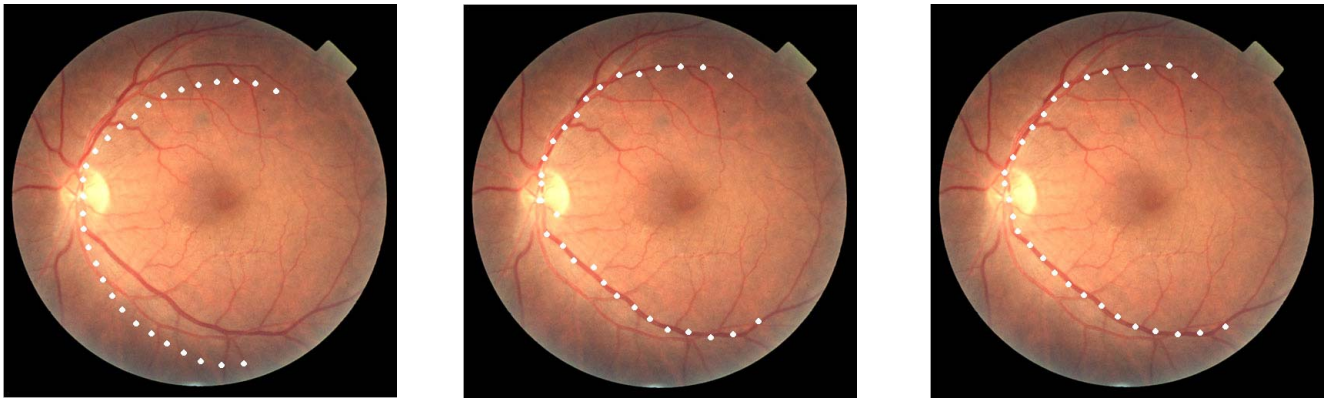

(a) Initialization of the shape model (b) The detected matching points (c) Main courses of blood vessels by the modified ASM

Figure 3: Extraction of the main courses of vessels by the modified ASM

We consider the extraction of the main courses of the blood vessels to locate fovea and establish fundus coordinate system. In the first approach, starting from the knowledge of optic disk location the modified ASM algorithm introduced in [12] was applied to extract the main courses of blood vessels. Here the shape of the main courses of blood vessels was represented by thirty landmark points. In the training images these points on the main vessels were annotated manually. An example of one of the training images with annotation of landmark points is illustrated in figure 1(a), with the corresponding shape instance shown in figure 1(b). The landmark points were selected evenly on the two central veins that were more obvious than arteries in the fundus images. Eight landmark sets were utilized as the training set. The training shapes were aligned to derive the Point Distribution Model (PDM). The variations of the shapes in the training images were found to be sufficiently described by the eigenvectors of the largest four eigenvalues, representing 94.27% of the variation in the training set. The model obtained from the training set for the left eyes and their first four modes are illustrated in figure 2 where the middle column shows the mean shape. The model for the right eyes were set to be symmetrical to that of the left eyes. The mean shape and the location of optic disk were used to initialize the shape model in the image space in the way similar to the one used in the boundary detection of optic disk. The modified ASM was applied to detect the shape instance of blood vessels in the image. The landmark points were matched to the centerline midpoint of the blood vessel with the strongest edge along the profile normal to the model boundary. One example of the blood vessel extraction is demonstrated in figure 3 where the initialization of the shape model in the image space is shown in figure 3(a). The matching points of the shape model are illustrated in figure 3(b) and the adjusted detection result of the main courses of blood vessels is demonstrated in figure 3(c).

The previous discussion is based on the assumption that the point (x_c, y_c) can be estimated from the knowledge of the optic disk size and its location. However this may not always be the case. When this piece of knowledge of the optic disk is not yet available the estimation of the convergence point of blood vessels can still be independently done and it has been satisfactorily shown to be the good estimate of the optic disk center. The procedure needs a basic reference to grouping of fundus photograph imaging according to the field of view it has been taken to display. Among seven standard fields [14] the first three fields are of particular interest to clinicians, and consequently to our work here. These are field 1 which is centered on the optic disk, field 2 centered on the macula, and field 3 temporal to the macula, including the fovea at 3:00 or 9:00 o'clock position. We can also segment the image into 3 regions - the upper region from the top of the image to 0.6 of the height of the image, the middle region that is 0.4 to 0.6 of the height of the image and lower region which is from 0.4 of the height of the image to the bottom of the image. In field 1, 2 and 3 fundus images, the optic disk is frequently found in the region 0.4 to 0.6 of the height of the image. Our method to identify the center of the optic nerve consists of two parts. First, we identify the main blood vessel by using the amplitude modified second-order Gaussian filter [15] with side-contrast checking. Then we track along the main blood vessel to a convergence point. The starting points for tracking to convergence in both the upper and lower region are the points nearest to the middle region. From the starting points, the one in the upper region will track down while the one in the lower region will track up using the tracking algorithm similar to that detailed in [16]. A step size of 4 is used for finer tracking with a search window of 3x3 to compensate for digitization error, all only in one iteration. Tracking from the upper and lower region proceeds alternately and independently until the stopping criteria are met. For instance, if tracking for the top region is stopped, the bottom region still continues until the stopping criteria are met or a convergence point is found. The convergence point is the midpoint between the upper and lower point if they are within a 30x30 neighborhood or if both are stopped before reaching this neighborhood, they must be within a 120x120 neighborhood. These windows are chosen after observing that the radius of optic disk is around 60 pixels for a 700x605 image.

Figure 4(a) shows the result of tracking to convergence point. As can be seen, there is no guarantee that the point will not track beyond the convergence point. Thus, an improved technique is implemented to take care of this problem.

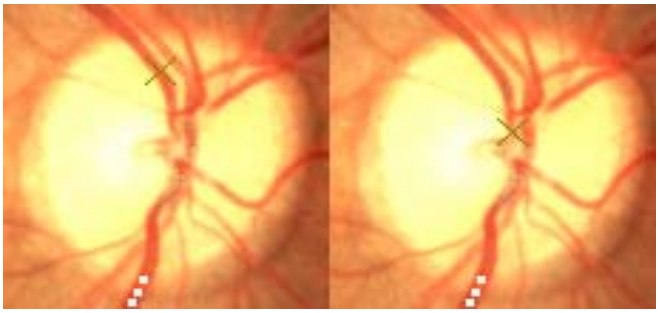

Figure 4: (a) The original tracking method. (b) The improved tracking method. Notice that the result is nearer to the optic nerve center.

- From the two starting points, a midpoint is calculated. If the midpoint is above the midline, i.e., a line that is at a position half the height of the image, the upper point will track only and vice versa.
- If tracking for upper point is terminated, this condition will be overruled and the bottom point will track only and vice versa.
- When the distance between the two points in the x or y direction is less than 30 pixels, both points will track together.
- When the two points are inside a 30x30 neighborhood, or a 120x120 neighborhood if both are terminated early, the midpoint is the center of the optic nerve.
- The process is repeated until the optic nerve is found or deemed to be unidentifiable or a maximum number of iteration is reached.

Notice that when the modified second-order Gaussian filter with tracking method is used, the modified ASM is no longer necessary. Out of 80 fundus images taken from the central hospital with resolutions ranging from 250×184 to 700×605 pixels and various degrees of pathologies, 69 of them had their optic disks successfully located within 60 pixels from the mean point identified by trained researchers. This represents a success rate of 86%. A recent work that offered a different and more complicated solution to this similar problem was presented by using fuzzy convergence [17].

III. Parabolic Fit To Blood Vessels

The two main courses of blood vessels together have their overall shape roughly like a parabolic curve. The extracted result is therefore fitted to a parabola for the subsequent estimate of the fovea location. When the rotation of the directrix is considered, the generalized parabola can be described as:

$$[(x-x_c)\sin\theta+(y-y_c)\cos\theta]^2 = 2p[(x-x_c)\cos\theta-(y-y_c)\sin\theta] \quad (1)$$

where $p/2$ is the focal length, (x_c, y_c) is the vertex of the parabola, and θ is the rotation angle of the directrix. Four parameters (p, x_c, y_c, θ) are to be estimated to describe the parabola shape in the image. The methods of quadratic curve fitting can be applied to this problem. As only thirty landmark points are obtained to describe the main courses of blood vessels, the least square fitting is more suitable than the clustering method such as Hough transform for fitting the landmark points to parabola. Since equation (1) belongs to a nonlinear model with respect to the parameters when the rotation of the directrix is considered, its parameters cannot be directly acquired by linear least square method. The voting concepts of Hough transform and linear least square fitting are then both employed in our case.

The procedure of fitting the main courses of blood vessels to parabola can be described as follows:

1. Estimation of (x_c, y_c) by setting it at half of optic disk radius in the nasal direction with respect to optic disk.
2. FOR θ from – 45° to 45° step 1
   FOR all the landmark points (x_i, y_i) in the main courses of blood vessels
   Translate and rotate their coordinates according to (x_c, y_c) and θ;
   $$x_i' = (x_i - x_c)\cos\theta + (y_i - y_c)\sin\theta$$
   $$y_i' = -(x_i - x_c)\sin\theta + (y_i - y_c)\cos\theta$$
   Calculate parameter p and the corresponding least square error e by least square fitting;
   $$p = \sum_{i=1}^{30} y_i'^4 \Big/ \left(2\sum_{i=1}^{30} x_i' y_i'^2\right)$$
   $$e = \sum_{i=1}^{30} \left[x_i' - (1/2p) y_i'^2\right]^2$$
3. Search the minimum e among the range of θ. Parameter p and θ are set to the corresponding value where minimum e is found.

IV. Fovial Localization

The fovea is a small depression on the fundus, which is indicated by a deep-red or red-brown color and a small brilliant reflex in the color fundus image. It is temporal to and slightly below the optic disk. There is a capillary-free zone of about 0.5mm corresponding to the fovea center [13]. The fovea is the darkest part in most of the fundus images, while it is not obvious to human eyes in some images due to high illumination or being covered by the lesions. Its geometrical relation to other structures is employed in this section to locate the fovea robustly.

After the structure of the main blood vessels has been obtained, the darkest region is searched to identify fovea. The candidate region of fovea is defined as the area of a circle having the radius of approximately one disk diameter (DD) with its center located at 2DD away from the disk center along the main axis of the fitted parabola. Because the fovea is situated about 2DD temporal to the optic disk in the fundus images [13], the candidate region is such defined in order to ensure that the fovea is within the region. An example of the foveal candidate region in a practical retinal image is demonstrated in figure 5 as the shaded area.

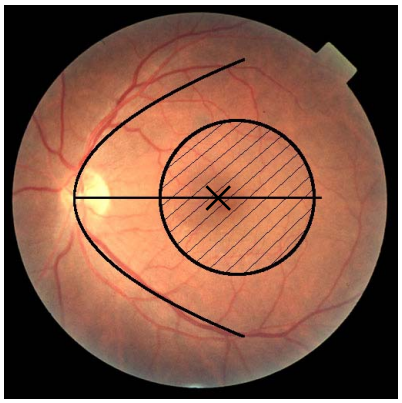

Figure 5: Results of fovea detection

The center of fovea is either detected as the darkest area in the candidate region or estimated as the center of the candidate region. The threshold is selected at the value below which the number of the pixels is the area of optic disk, because the fovea is about the same size as optic disk [13]. The pixels with intensity below the threshold and within the distance of 1DD are clustered and the region that has the lowest mean intensity is found. The lowest mean intensity is compared with the second lowest mean intensity to ensure the correct detection. Since the fovea is not obvious in some images, the comparison is performed in

order to avoid mistaking the peripheral area where the illumination is relatively dark in the candidate region as fovea. If the difference is obvious and the number of pixels in the cluster is greater than 1/6 disk area, the centroid of the cluster with the lowest mean intensity is located as the center of fovea. The fovea is estimated at 2DD temporal to the center of optic disk along the main axis of the fitted parabola when the difference is small. Figure 5 presents the result of fovea detection by the centroid of the cluster with the lowest mean intensity. Thirty-five color fundus images have been tested by the proposed algorithm to locate the fovea. The fovea is detected directly by the centroid of the darkest region in twenty-one of the images and it has to be estimated in the other fourteen images as the fovea is not obvious in the latter group. The localization of the fovea is within the region of fovea in all these thirty-five images but it slightly deviates from the foveal center in three of the fundus images when evaluated by the human eyes. The localization of fovea is then estimated in all of these three images. The reason of the deviation between the localization and the foveal center is that the estimate of two disk diameters away from disk center may not be precise.

ACKNOWLEDGMENT

The author thanks reviewers for their many valuable suggestions.

V. CONCLUSION

The localization of fovea in fundus image has been described in this paper. One is based on the modeling of main blood vessel profile and the modified ASM when the location of the optic disk and the retinal data has been modeled *a priori*; another one is based on a modified-Gaussian matched-filter tracking method when the optic disk location is not known. Among various results a tracking strategy to improve the optic disk localization and an effective parabolic curve fitting by a method of least square fitting and voting are some contributions presented here. The foveal center is detected as the centroid of the darkest cluster in the candidate region determined by the spatial relationship of the optic disk and the structure of blood vessels. When the detection fails, it is estimated according to its geometrical relationship to other features in the fundus image. The foveal fundus coordinates can then be subsequently established and the spatial relationship between lesions and landmark features easily described.

REFERENCES

[1] T. Teng, M. Lefley, and D. Claremont, "Progress towards automated diabetic ocular screening: a review of image analysis and intelligent systems for diabetic retinopathy," *Med. & Biol. Eng. & Comput.,* vol. 40, pp 2-13, 2002.

[2] ETDRS Report Number 10, "Grading diabetic retinopathy from stereoscopic color fundus photographs-An extension of the modified Airlie house classification," *Ophthalmology*, vol.98, pp.786-806, 1991.

[3] H. Li and O. Chutatape, "Fundus image features extraction," in *Proc. 22nd Annu. IEEE Int. Conf. Engineering in Medicine and Biology Society*, vol. 4, pp.3071 -3073, 2000.

[4] S. Chaudhuri, S. Chatterjee, N. Katz, M. Nelson and M. Goldbaum, "Detection of blood vessels in retinal images using two-dimensional matched filters," *IEEE Trans. Med. Imag.*, vol. 8, pp.263-269, 1989.

[5] Y. Wang and S. C. Lee, "A fast method for automated detection of blood vessels in retinal images," in *Proc. 31th Asilomar Conf. Signals, Systems & Computers*, vol. 2, pp.1700-1704, 1997.

[6] S. Tamura, Y. Okamoto and K. Yanashima, "Zero-crossing interval correction in tracking eye-fundus blood vessels," *Pattern Recognit.*, vol. 21, no. 3, pp.227-233, 1988.

[7] B. Kochner, D. Schuhmann, M. Michaelis, G. Mann and K. H. Englmeier, "Course tracking and contour extraction of retinal vessels from color fundus photographs: Most efficient use of Steerable filters for model based image analysis," in *Proc. SPIE Conference on Image Processing*, pp.755-761, 1998.

[8] O. Chutatape, Z. Liu and S. M. Krishnan, "Retinal blood vessel detection and tracking by matched Gaussian and Kalman filters," *Proc. 20th Annu. Int. Conf. IEEE Engineering in Medicine and Biology Society*, pp.3144-3148, 1998.

[9] R. Giansanti, P. Fumelli, G. Passerini, and P. Zingaretti, "Image system for retinal change evaluation," *IEE Proc. Conf. Image Processing and Its Applications*, vol. 2, pp. 530-534, 1997.

[10] C. Sinthanayothin, J. F. Boyce, H. L. Cook and T. H. Williamson, "Automated location of the optic disk, fovea, and retinal blood vessels from digital colour fundus images," *Br. J. Ophthalmol.*, vol. 83, no. 8, pp.902-910, 1999.

[11] G. G. Gardner, D. Keating, T. H. Williamson, and A. T. Elliott, "Automatic detection of diabetic retinopathy using an artificial neural network: A screening tool," *Br. J. Ophthalmol.*, vol. 80, no. 11, pp.940-944, 1996.

[12] H. Li and O. Chutatape, "Automatic Location of Optic Disk in Retinal Images," in *Proc. IEEE In. Conf. Image Processing*, Thessaloniki, Greece, vol. 2, pp 837-840, October 2001.

[13] H. W. Larsen, *The Ocular Fundus: a Color Atlas*, 1976.

[14] (Online Source) Available: http://eyephoto.ophth.wisc.edu/Photography/Protocols/AIDS/AIDSPhotoProtocol.html

[15] L. Gang, O. Chutatape, and S. M. Krishnan, "Detection and Measurement of Retinal Vessels in Fundus Images Using Amplitude Modified Second-Order Gaussian Filter," *IEEE Trans. Biomedical Engineering*, vol 49, no 2, pp 168-172, 2002.

[16] H. K. Lam and O. Chutatape, "Blood vessel tracking technique for optic nerve localisation in field 1 and 2 color fundus images," in *Proc. 4th Int. Conf. Information, Communications & Signal Processing and 4th Pacific-Rim Conf. Multimedia*, Singapore, Dec. 2003.

[17] A. Hoover and M. Goldbaum, "Locating the optic nerve in a retinal image using the fuzzy convergence of blood vessels," *IEEE Trans. Medical Imaging*, vol 22, pp 951-958, 2003.